



24

25 **INTRODUCTION**

26 The presence of vegetation in open channels and in environmental aquatic flows has been  
27 recognized to be important for the balance of river ecosystems, e.g., through the provision of  
28 river restoration and stabilization of channels (Lopez and Garcia, 1998). To predict  
29 accurately the conveyance capacity in open channels, it is important to understand the  
30 hydrodynamic interaction of the flow with the boundary.

31 Changes in the shape or resistance characteristics of a channel boundary can induce a change  
32 in the flow characteristics (Jesson et al., 2013). The velocity profile can become distorted  
33 with shear being created at the interface between roughness elements, leading to additional  
34 sources of turbulence. Jesson et al. (2012) investigated the effect that changes in bed  
35 roughness can have on the mean and turbulence characteristics of the velocity field. This  
36 work highlighted the importance that the rough-smooth boundary (i.e., the location where the  
37 bed roughness changed) has on the overall momentum transfer and vorticity generation. The  
38 research outlined below, extends the work of Jesson et al. (2013) by considering the effect  
39 that idealised vegetation can exert on the main flow characteristics in a heterogeneous  
40 channel. In what follows, a detailed investigation of the flow characteristics will be presented  
41 for the particular case where the channel bed is composed of heterogeneous roughness  
42 formed using gravel and idealised vegetation. However, before these results are presented it  
43 is worth briefly considering the fundamental basics of canopy flow since this will provide a  
44 framework in which the results can be interpreted.

45 The distribution of vegetation elements within a canopy can significantly affect the  
46 behaviour of the flow (Nepf, 2012). In a sparse canopy (see Figure 1 for definition), the  
47 velocity follows a turbulent boundary layer profile with the bed contributing to the vegetation  
48 roughness (Nepf, 2012). In a dense canopy (Figure 1c), the vegetation drag is larger than the

49 bed shear stress; the flow at the top of vegetation produces a free shear layer through an  
50 inflection point near the top of the canopy which leads to flow instability and the additional  
51 creation of vortices (Ghisalberti and Nepf, 2002, 2006, Nepf, 2012). The vegetation stem  
52 density defines the transition from sparse to dense limits with scale  $ah$ , where  $a$  is the stem  
53 frontal area, and  $h$  is the vegetation height.

#### 54 **AIMS AND OBJECTIVES**

55 Despite the excellent work undertaken by Nepf (2012) and Jesson et al., (2010; 2012; 2013),  
56 the interaction of vegetation with other forms of roughness is still poorly understood. Hence,  
57 the overall aim of the current research, is to evaluate how the dynamics of the flow field  
58 change when heterogeneous roughness involving vegetation is present. Related to this the  
59 research has the following objectives:

- 60 • To investigate the influence that rigid vegetation (akin to ‘shrubs’) and flexible  
61 vegetation (akin to ‘grass’) have on turbulence generation within an open channel.
- 62 • To investigate the influence of vegetation distribution on the velocity shear and  
63 turbulence generation

#### 64 **EXPERIMENTAL METHODS**

65 The experiments were conducted in 22mm long rectangular re-circulating flume of width  
66  $B = 614mm$  at the University of Birmingham. The channel is supplied from a constant head  
67 tank with a capacity of 45,500l in the laboratory roof. Two flow discharges ( $Q$ ) were  
68 investigated (30.0 l/s and 30.50 l/s) with corresponding flow depths ( $H$ ) of 130mm and  
69 128mm and width to depth ratios ( $B/H$ ) of 4.7 and 4.8 respectively to achieve subcritical  
70 flow condition. In what follows these experimental conditions are referred to as EXPT1 and  
71 EXPT2 respectively. The corresponding water surface slopes for EXPT1 and EXPT2 were

72 0.0008 and  $0.0011 \pm 0.0001$  respectively. Detailed velocity measurements were made at  
73 three cross sections (CRS1, CRS2 and CRS3) at distances of 17.5m, 17.85m and 18.2m  
74 respectively downstream from the channel inlet. In the results that follow, the gravel region  
75 of the bed extends over  $(0 \leq y/B \leq 0.5)$ , the interface occurs at  $(y/B = 0.5)$ , and the  
76 vegetated region extends over  $(0.5 \leq y/B \leq 1.0)$ , where  $y$  is the lateral distance from the  
77 left hand side looking downstream and  $B$  is the channel width. The streamwise direction  $x$  is  
78 in the direction of flow. The transverse direction  $y$  is perpendicular to  $x$  in the lateral  
79 direction, while the vertical direction is denoted by  $z$  and is perpendicular to the  $xy$  plane  
80 (positive upwards). The corresponding time average velocity components are  $U, V, W$   
81 respectively with the associated fluctuating velocity components defined as  $u', v', w'$   
82 respectively.

### 83 **Vegetation Types and Roughness Generation**

84 Two different types of idealised vegetation are examined in conjunction with the gravel  
85 roughness ( $D_{70}=10mm$ ), i.e., idealised grass formed using artificial grass (Astroturf) and rigid  
86 vegetation arranged in a staggered grid formed from plastic (see Table 1 and Figure 2). In  
87 keeping with the work of Jesson et al. (2013) the vegetation and gravel form patches of width  
88 0.307m and length 1.825m and alternate in a checkerboard formation down the channel  
89 (Figure 2).

90 **Table 1: Summary of vegetation roughness properties**

	Height	Width	Thickness	Density
<b>EXPT1-Grass</b>	26mm	1mm	0.15mm	15625plants/m <sup>2</sup>
<b>EXPT2-Rigid</b>	26mm	15mm	10mm	800plants/m <sup>2</sup>

91 **Data collection**

92 ***Velocity Measurement***

93 Velocity measurements were undertaken at all three cross sections (CRS1, CRS2, and CRS3),  
94 using a Nortek acoustic Doppler velocimeter (ADV) and 4mm diameter Pitot static tube for  
95 the free surface and within the vegetation. The ADV measures simultaneously the three  
96 velocity components at a frequency of 200Hz. A convergence test was performed to obtain an  
97 optimum sampling period at each measurement point (i.e., 60 seconds). For each cross  
98 section a vertical profile of velocity data was collected from the middle of the channel  
99 towards the channel sidewalls at 10mm horizontal and vertical spacing resulting in  
100 approximately 495 measured points for a cross section. For each vertical profile the  
101 maximum measurable height with ADV was 5cm below the free surface.

102 **RESULTS**

103 **Mean velocity Profiles and Distribution**

104 The mean velocity ( $U_m$ ) was obtained for each measured point and normalized by the bulk  
105 mean velocity ( $U_{Q/A}$ ) where  $A$  is the cross sectional area. To provide an indication of the  
106 degree of reliability of the data collected, the time averaged velocity data at each point was  
107 numerically integrated and compared to  $U_{Q/A}$ . For EXPT1 and EXPT2 the difference was 3%  
108 and 2.8% respectively; this was considered appropriate for the current work and is  
109 comparable with Jesson et al. (2013).

110 Figure 3 shows transverse profiles of streamwise velocity for selected elevations. With  
111 regards to EXPT1 the grass vegetation retards the transverse profiles relative to gravel bed,  
112 while the minimum averaged velocity appears at the roughness interface region in EXPT2.  
113 Generally it can be seen that all transverse profiles indicate a change in lateral shear (i.e.

114 changes in  $dU/dy$  at the interface ( $y/B = 0.5$ ) between the gravel and vegetated sections. As  
115 indicated in Figure 3, increased lateral shear is more pronounced in EXPT1 (artificial grass)  
116 compared to the EXPT2 (rigid boundary). What is also interesting is the indication in EXPT2  
117 that the gravel surface is rougher than the rigid vegetation.

118 Figure 4 compares the vertical mean velocity ( $U_m$ ) profiles for three cross sections over the  
119 vegetated and gravel bed. It can be seen from the figure that the presence of vegetation  
120 retards the flow near bed with much lower value over the vegetated region ( $y/B = 0.65$ )  
121 relative to gravel region ( $y/B = 0.19$ ) in EXPT1. This is attributed to the slow velocity flow  
122 within the vegetation due to stem density and the resulting vertical shear as further examined  
123 in the subsequent results. In EXPT2, the mean velocities are approximately constant over a  
124 large proportion of the two bed roughness at a given height as illustrated in Figure 4. The  
125 effect of the near bed accelerated flow on the vertical shear in EXPT2 is given in the  
126 discussion section.

127 The vertical profiles of the mean velocity over vegetated bed is explored further to examine  
128 the flow existence within the vegetated bed, measurements were undertaken for three vertical  
129 points using a Pitot - static tube 4mm diameter. The vertical velocity profiles are shown in  
130 Figure 5. Vegetation stems were removed within an area  $0.03m^2$  to allow the tube into  
131 vegetation zone. The flow within the vegetation is at a smaller spatial scale ( $z/H \leq 0.07$ ) but  
132 the measurements revealed low velocities compared to the value at the vegetation top as  
133 measured using the ADV forming two layer flows over vegetated bed given an indication of  
134 vertical shear. The analysis of the dynamics of vertical with horizontal shear is given in the  
135 discussion section.

136 Figure 6 shows the secondary flow distributions for EXPT1 and EXPT2. The maximum  
137 measured secondary flow vector is within 3% of the mean streamwise velocity for both  
138 experiments and is in keeping with the findings of Jesson et al., (2012 and 2013). Visual  
139 inspection shows that the magnitude of secondary flow over the gravel bed in EXPT1 is large  
140 with occurrence of down-flow, and up-flow over the grass bed. At the lower region ( $z/H \leq$   
141  $0.2$ ) of the flow, the transverse motion is directed from the gravel bed towards the grass bed,  
142 and at the upper region ( $z/H > 0.2$ ), the flow is transported laterally in opposite direction. The  
143 secondary flow vectors in EXPT2 suggest the presence of circulating cells moving in  
144 clockwise direction (Jesson et al., 2013, Jesson. et al., 2012, Knight et al., 2007, Nezu and  
145 Nakagawa, 1984, Wang and Cheng, 2005), with a strong up-flow at the roughness  
146 interface ( $y/B = 0.5$ ), the flow cells in clockwise direction appear to dominate momentum  
147 transfer between the bed strips Figure 6. The up-flow corresponding to the low velocity flow  
148 over vegetated region in Figure 4 may be caused by the retardation of the flow near bed by  
149 the grass vegetation.

### 150 **Profiles of Reynolds Stress**

151 Figure 7 compares the vertical profiles of vertical Reynolds stress ( $-\overline{u'w'}/\tau_b$ ) where  $u'$  and  
152  $w'$  are streamwise and vertical fluctuating velocities respectively. The mean boundary shear  
153 stress  $\tau_b$  was evaluated as  $\rho g R S_0$  where  $\rho$  is the water density,  $g$  is the acceleration due to  
154 gravity,  $R$  is the hydraulic radius and  $S_0$  is the bed slope. Over the gravel bed ( $0 \leq y/B \leq$   
155  $0.5$ ), the vertical Reynolds stress has a local maximum above the bed at  
156 approximately ( $z/H \cong 0.2$ ), after which it decays in approximately linear fashion towards the  
157 channel bed and the free surface from the maximum point. This is in good agreement with the  
158 wall region as defined by (Nezu and Nakagawa, 1993). In this region the vertical Reynolds  
159 stress decreases towards the channel bed due to the presence of non-negligible viscous shear

160 stress induced by the bed surface (Nezu and Nakagawa, 1993). Moreover, the near bed  
161 momentum transport from gravel bed to the vegetated bed is assumed to have contributed to  
162 the reduced value of the near bed shear stress over the gravel bed. This is observed to have  
163 contributed to the momentum balance in the near bed flow region (Shiono and Knight, 1991)

164 Over the vegetated bed ( $0.5 \leq y/B \leq 1.0$ ), the vertical Reynolds stress is reasonably linear  
165 over the measured section, with a maximum value occurring close to the channel bed. This  
166 behaviour is consistent with an inflection point in a submerged vegetation which is  
167 characterized by a shear layer and possibly indicates the existence of a ‘wake layer’ below  
168 the vegetation surface roughness as shown in Figure 5; thus, the effective height of the bed  
169 lies below the roughness crest (Nezu and Nakagawa, 1993),

170 Figure 8 shows contours of the horizontal Reynolds stress ( $-\overline{u'v'}/\tau_b$ ) where  $v'$  is the lateral  
171 fluctuating velocity. The figure indicates the existence of the horizontal Reynolds stress over  
172 the vegetated bed. The shear propagation across the bed and towards the gravel zone is  
173 apparent; this may be attributed to the vertical orientation of vegetation stems enhancing  
174 small scale horizontal turbulence due to stem wakes within vegetation. Comparing Figure 6  
175 and Figure 8, it can be seen that the region of maximum (negative) horizontal Reynolds stress  
176 correspond with the up-flow regions.

177

178 In addition, the horizontal Reynolds stress is maximized at the roughness interface region

179 ( $y/B = 0.5$ ) of the flow in EXPT2.

## 180 **DISCUSSION**

### 181 **Vegetated and Roughness Interface Shear Layer Flow**

182 The dominant factor influencing turbulent transport in open channel flow is the degree of  
183 velocity shear due to different roughness sections. In this paper, Reynolds stresses are  
184 assumed as indicators of turbulence transport effects (Shucksmith et al., 2010).

185 The presence of both vertical and horizontal shear is notable in this work from Figures 3 and  
186 5; efficient vertical transport of momentum across the shear layer through the vegetation-  
187 water interface region ( $z/H \leq 0$ ) relative to gravel bed is expected due to the vertical shear  
188 over the vegetated bed as shown in Figure 5. Similarly, there is evidence of horizontal shear  
189 at the roughness interface regions ( $y/B = 0.5$ ) as shown by the lateral velocity profiles. In  
190 such condition turbulence transfer is expected over the roughness interface region.

191 Referring to Figure 7, the vertical profiles of Reynolds stress exhibit a strong peak at the  
192 position of the vegetation top; this height coincides with the inflection point in the velocity  
193 profile in Figure 5. The shear layer is featured in this work by the point of the maximum  
194 Reynolds stress at the top of vegetation as shown in the vertical distributions of the vertical  
195 Reynolds stress in Figure 7. It should be noted from the figures that the vertical Reynolds  
196 stress exhibits more peak over the vegetated bed in EXPT1 than in EXPT2.

197 Figure 9 compares the depth averaged vertical and horizontal shear stresses. The figure  
198 illustrates greater magnitude of vertical shear over the vegetated grass bed relative to the  
199 gravel bed in EXPT1; this is assumed to enhance turbulence in the vertical plane due to  
200 increased vegetation density. Also noted is the negative lateral momentum transport at the  
201 interface region ( $y/B = 0.5$ ), the vertical shear over vegetated bed in EXPT1 is assumed to

202 have suppressed the level of horizontal shear at the interface region in contrast to Jesson et  
203 al., (2012) where the momentum transfer is maximized at the rough-smooth boundary.

204 In EXPT2, the horizontal turbulent shear stresses attain a maximum at the roughness interface  
205 region ( $y/B = 0.5$ ) which is consistent with the results in figures 6 and 8.

## 206 **Bursting Mechanism by Quadrant Analysis**

207 To investigate the coherent structure due the multiple shear layer induced by vegetation, a  
208 quadrant conditional analysis as proposed by (Nakagawa and Nezu, 1977) for instantaneous  
209 Reynolds stress is applied. The quadrant Reynolds stress  $QR_i$  is defined as follows:

210

$$211 \quad QR_i = \lim \frac{1}{T} \int_0^T (u'(t) \cdot v'(t)) I(t) dt \quad (i = 1, 2, 3, 4) \quad (2)$$

212

213 The quadrant analysis divides the paired time series data into four quadrants based on the  
214 signs of the fluctuating velocity components. In this research the following analyses describes  
215 the pair of streamwise velocity fluctuation ( $u'$ ) and vertical velocity fluctuation ( $w'$ )  
216 components in each quadrant. The existence of pair fluctuating components ( $u', w'$ ) defines  
217 event in quadrant  $i$ ,  $I$  provides indication of right event in a quadrant  $i$ . If fluctuating  
218 components ( $u', w'$ ) exists in a quadrant  $i$ , then  $I_i = 1$ , otherwise  $I_i = 0$ . Each quadrant is  
219 defined for the following events:

220

221  $i = 1 (u' > 0, w' > 0)$ : Outward interaction of high velocity

222  $i = 2, (u' < 0, w' > 0)$ : Ejections of low velocity flow

223  $i = 3, (u' < 0, w' < 0)$ : Inward interactions of low velocity flow

224  $i = 4 (u' > 0, w' > 0)$ : Sweep

225 Figure 10 show the vertical distributions of the quadrant Reynolds stress  $Q_i$  normalized by  
226 the bulk shear stress for selected sections over gravel bed ( $y/B = 0.24$ ) and vegetated  
227 bed ( $y/B = 0.73$ ) for EXPT1 and EXPT2 respectively. The Reynolds stress contribution  
228 analysis demonstrates that ejection ( $Q_2$ ) and sweep ( $Q_4$ ) events are the most evident  
229 dominant contributors to the Reynolds shear stress. This observation is consistent with the  
230 previous research works (Nezu and Nakagawa, 1993). However the contributions of ( $Q_1$ ) and  
231 ( $Q_3$ ) events are predominantly negative. In EXPT1 Figure 10 (top), the distributions of  
232 sweep ( $Q_4$ ) and ejection ( $Q_2$ ) have their maximum values over the gravel and the vegetated  
233 bed, Ejection motions ( $Q_2$ ) dominates Sweep motions over grass vegetated bed by exhibiting  
234 much larger value than Sweep ( $Q_4$ ) over the grass vegetated bed, it should be noted that the  
235 Ejection motions transport the low velocity flow over the grass bed up to the free surface, this  
236 supports the upward secondary flow as observed in Figure 6, and over the gravel bed the  
237 Sweep motions dominates Ejection motions. At the upper region of the flow, Ejection  
238 motions generally dominate the flow and turbulence transport. Similar distributions are  
239 observed in EXPT2 where Ejections and Sweeps dominate the flow Figures 10 (down). The  
240 Sweep motions are more significant near bed while Ejections dominates the flow at the upper  
241 region of the flow. In both experiments, the contributions of the inward ( $Q_1$ ) and outward  
242 ( $Q_3$ ) interactions are negligibly small and negative. This result implies that Ejection and  
243 Sweep events are most evident in similar manner as observed in boundary layer problems in  
244 open channel flows. Relative to EXPT1, the peak values of Ejection ( $Q_2$ ) in EXPT2 becomes  
245 smaller; this supports the observation of smaller vertical momentum exchange in EXPT2 in  
246 comparison to EXPT1. It has been observed in the literature (Nepf and Ghisalberti, 2008) that  
247 vertical shear layer generation is directly proportional to the density and distribution of  
248 vegetation elements.

249 **CONCLUSIONS**

250 This research extends the work of Jesson et al., (2010; 2012; and 2013) by considering the  
251 effect of idealized vegetation on the flow characteristics of a heterogeneous open channel.  
252 The study present results of experiments with two different types of idealised vegetation  
253 patches with gravel roughness. In EXPT1 idealised grass is formed using artificial grass  
254 (Astroturf) and rigid vegetation arranged in a staggered grid formed from plastic material in  
255 EXPT2.

256 The research has highlighted the following based on the objectives;

- 257 • The vertical profiles of the mean velocity show lower mean velocities near bed over  
258 vegetated bed in EXPT1 as shown in Figure 4, furthermore it is shown in Figure 5  
259 that the grass stem density increases the retardation of the flow within the vegetation.  
260 Therefore the magnitude of the velocity difference within and over the vegetation  
261 become more effective in promoting vertical turbulence
- 262 • In keeping with the previous work (Jesson. et al., 2012), the lateral interaction and  
263 transport is achieved by the secondary flow, at the lower region ( $z/H \leq 0.2$ )of the  
264 flow, the transverse motion is directed from the gravel bed towards the grass bed, and  
265 at the upper region ( $z/H > 0.2$ ), the flow is transported laterally in the opposite  
266 direction in EXPT1. The secondary vector in EXPT2 suggests the presence of  
267 circulating cells moving in clockwise direction as illustrated in Figure 6.
- 268 • In EXPT1, the presence of vegetation promotes vertical shear and the resulting  
269 dominance of vertical momentum transport as illustrated in Figure 7. Applying a force  
270 balance to the depth averaged the momentum equation; the dominance of vertical  
271 momentum transport over the vegetated bed is shown to suppress the lateral  
272 momentum transport at the roughness interface ( $y/B = 0.5$ )as shown in Figure 9.

- 273 • In EXPT2, the distribution of the vegetation elements to achieve a staggered pattern  
274 created less a dense flow domain within the vegetation which reduced the vertical  
275 shear over the vegetated bed relative to EXPT1 (Figure 5). This is assumed to  
276 enhance the lateral momentum transfer at the roughness interface region similar to  
277 Jesson et al., (2013) as illustrated in Figure 8 and 9. This indicates that the roughness  
278 distribution has an enhanced impact on turbulence generation compared to the  
279 magnitude of the surface roughness.
- 280 • As shown in Figure 7, the velocity shear and turbulence resulting from the boundary  
281 effect over the gravel bed are dominated by the vegetation generated turbulence.
- 282 • The study demonstrates that relative to turbulence distribution, the vegetated bed  
283 exerts a major influence on the flow.
- 284 • From the results, local regions of efficient moment transport can be predicted in  
285 natural rivers with similar patches of roughness.

286 **Acknowledgements**

287 Financial support was provided by the Tertiary Education Fund (TETFUND) Nigeria.

288 Authors graciously acknowledge and appreciate the support.

289

290

291

292

293

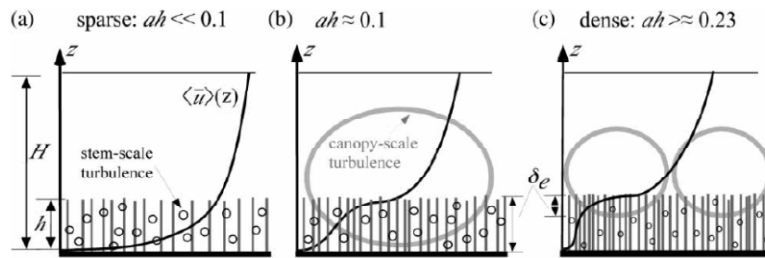
294

295

296

297

298  
 299  
 300  
 301  
 302  
 303  
 304  
 305 **Figures**

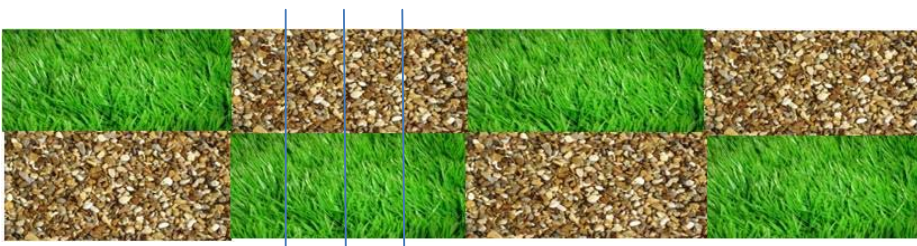


306  
 307  
 308

Figure 1: The mean velocity profiles in submerged vegetation with increasing stem density (Nepf, 2012)



309



310

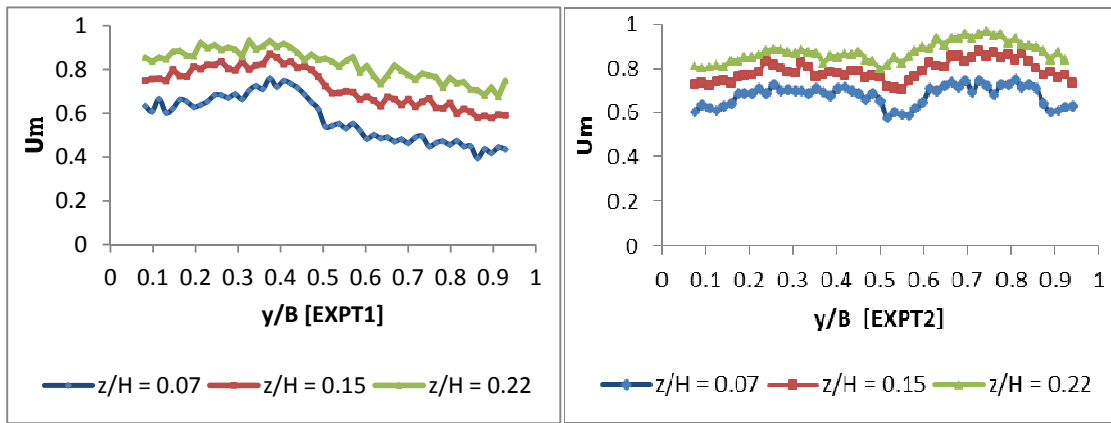
CRS1 CRS2 CRS3

311

312 **Figure 2: Two model vegetation simulated with gravel roughness: EXPT1( left upper); EXPT2 (right upper) and the**  
 313 **plan view showing the three cross sections measured.**

314

315



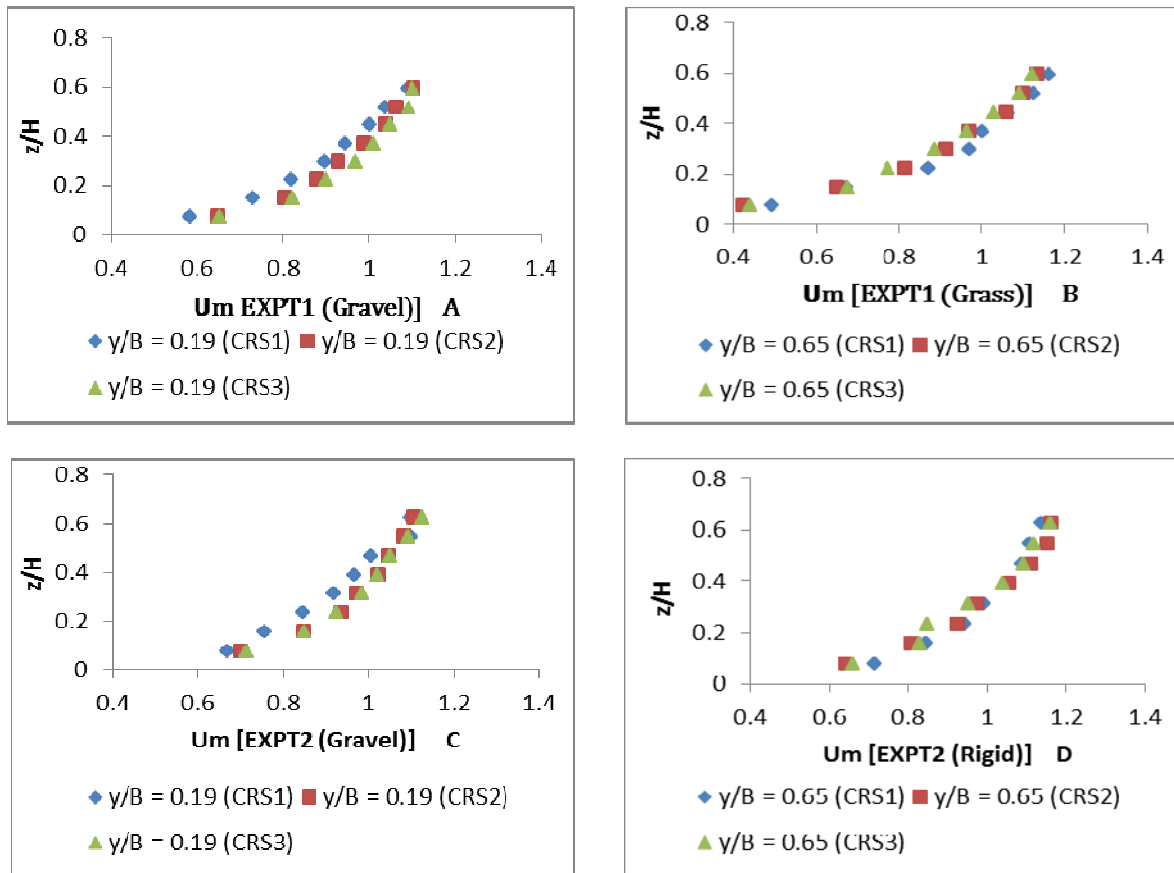
316

317

Figure 3: Lateral velocity profiles CRS3: (a) EXPT1, (b) EXPT2.

318

319

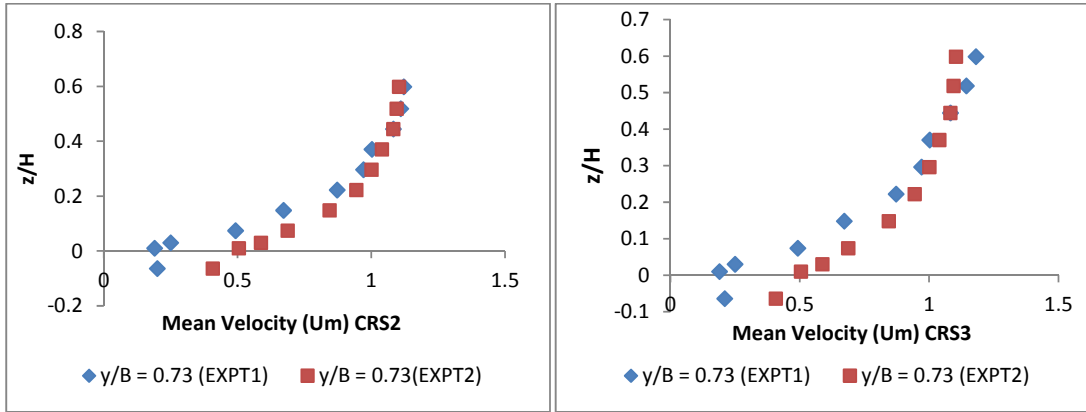


320

321

Figure 4. Selected vertical profiles of mean velocity from CRS1, CRS2 and CRS3: EXPT1 and EXPT2.

322



323

324

Figure 5: Vertical velocity profiles over vegetated bed with porous layer for cross section one and two

325

326

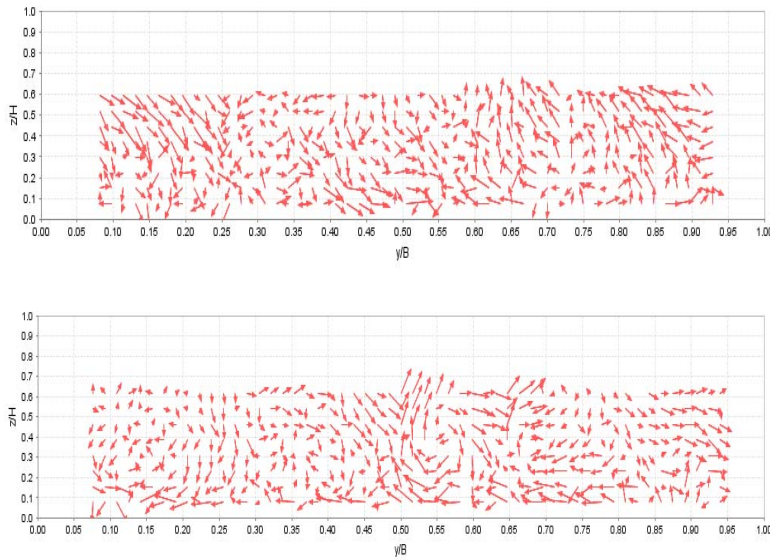
327

328

329

330

331



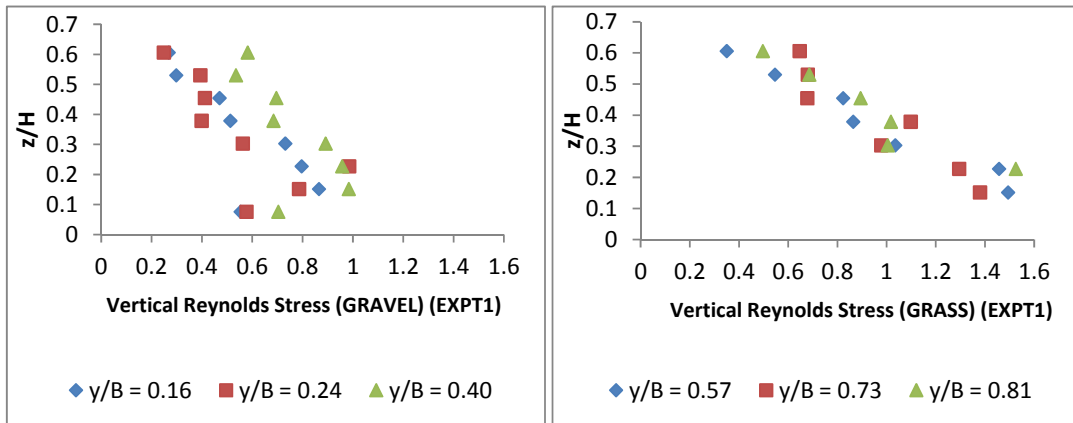
332

333

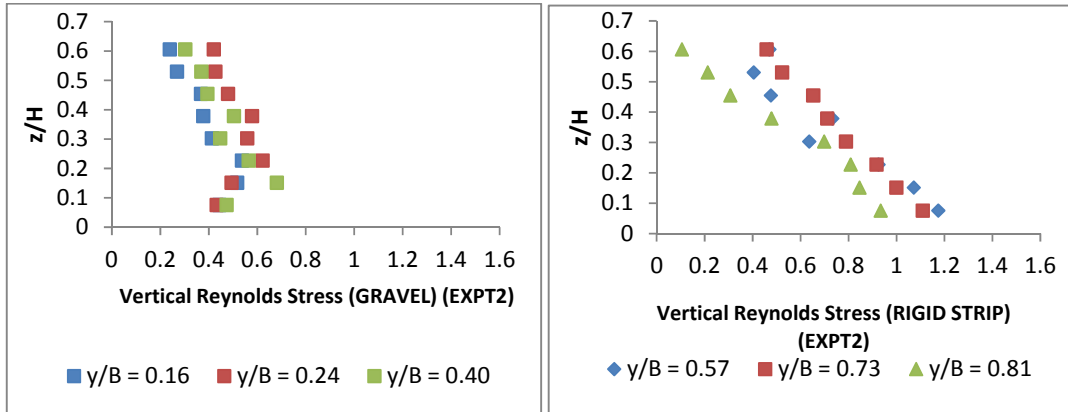
Figure6: Secondary flow distribution CRS3: EXPT1 (upper), EXPT2 (lower)

334

335



336



337

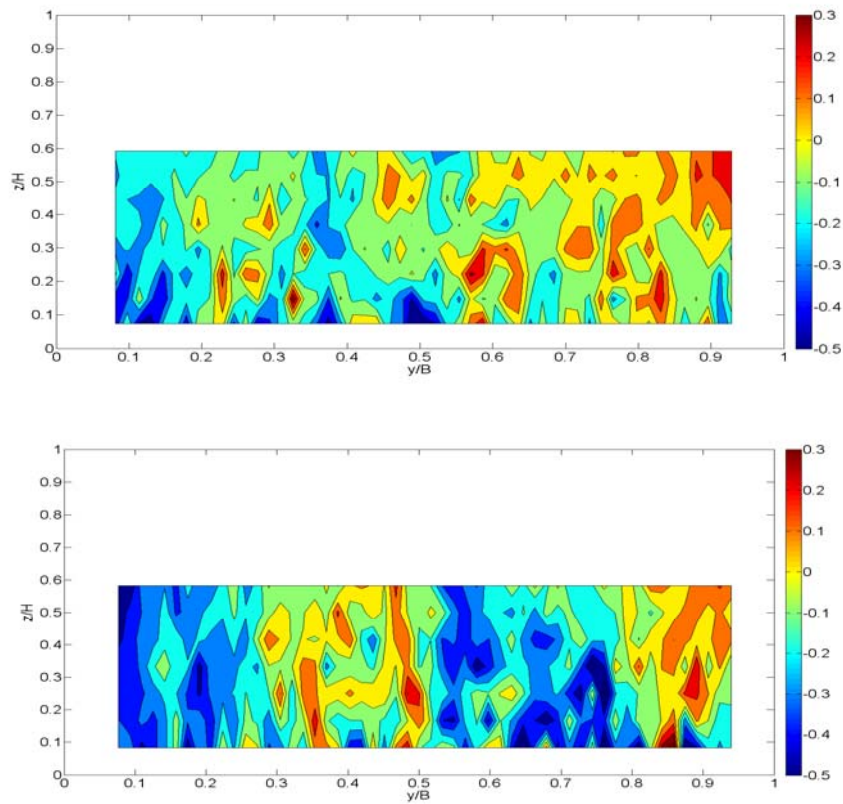
338

Figure 7: Vertical profiles of Vertical Reynolds stress by bed: EXPT1 (top), EXPT2 (down)

339

340

341



342

343

344

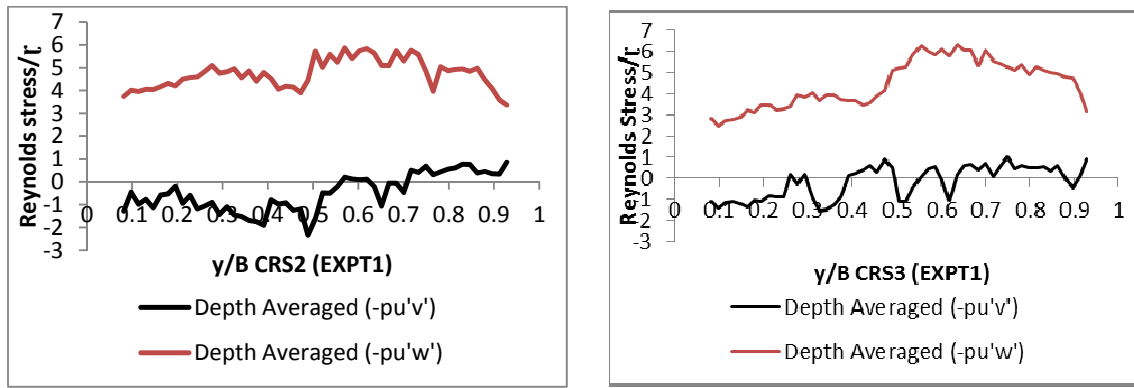
Figure 8: Distribution of Relative Horizontal Reynolds stress: EXPT1 (upper), EXPT2 (lower)

345

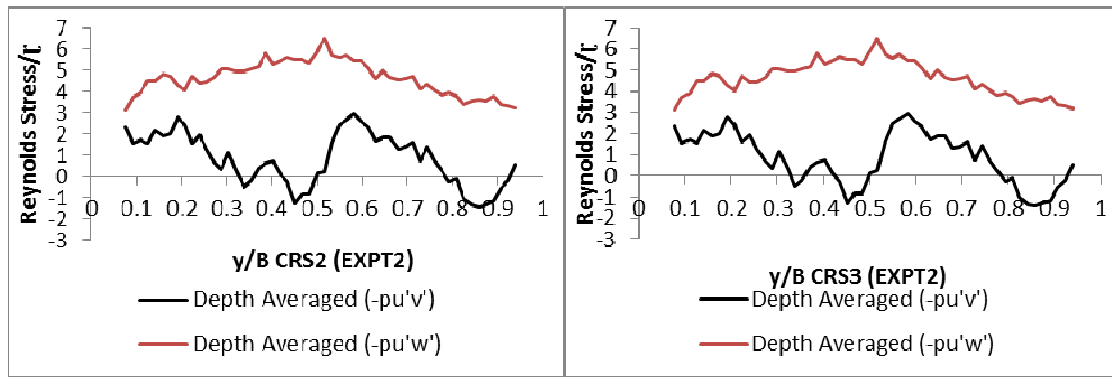
346

347

348



349



350

Figure 9: Lateral Distribution of depth averaged horizontal and vertical shear stresses for EXPT1 and EXPT2.

351

352

353

354

355

356

357

358

359

360

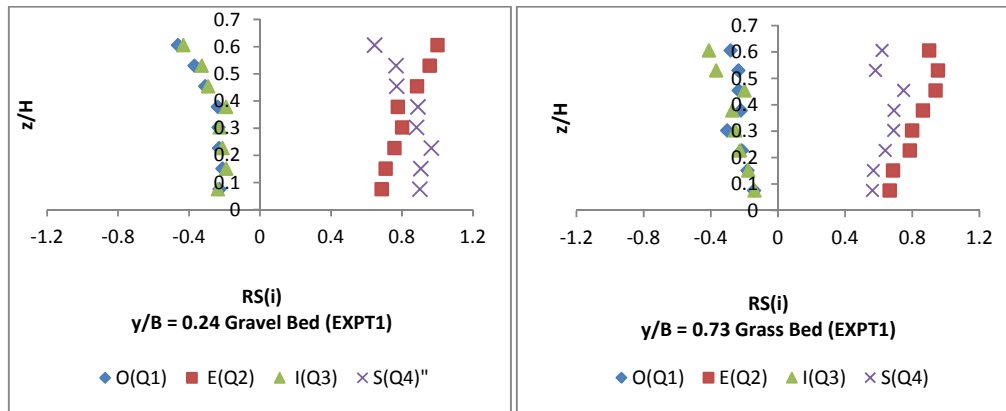
361

362

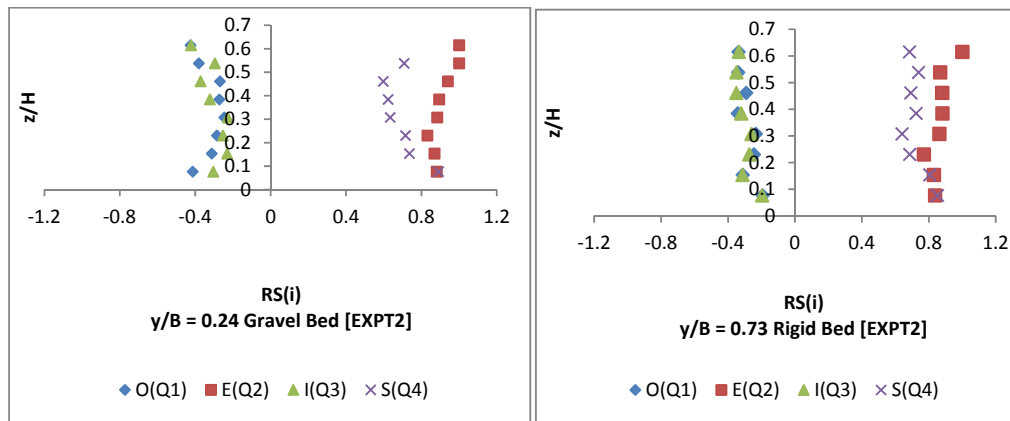
363

364

365



366



367

Figure2: Quadrant Reynolds Stress distribution over gravel and vegetated beds: EXPT1 ( top), EXPT2 (down)

368

369

## REFERENCES

370

Ghisalberti, M. and Nepf, H.M. (2002) Mixing layers and coherent structures in vegetated aquatic flows. **Journal of Geophysical Research**, 107: (C2).

371

372

Ghisalberti, M. and Nepf, H.M. (2006) The structure of shear layer flow flows over rigid and flexible canopies. **Environ Fluid Mech**, 6: (3): 277-301.

373

374

Jesson, M., Sterling, M. and Bridgeman, J. (2013) Modelling Flow in an Open Channel with Heterogeneous Bed Roughness. **Journal of Hydraulic Engineering**, 139: 195-204.

375

376

Jesson., M., Sterling M. and Bridgeman, J. (2012) An experimental Study of Turbulence in a Heterogeneous Channel. **Water Management Proceedings of the Institution of Civil Engineers**, 166: (WM1): 16-26.

377

378

379

Knight, D.W., Omran, M. and Tang, X. (2007) Modeling Depth-Averaged Velocity and Boundary Shear in Trapezoidal Channels with Secondary Flows. **Journal of Hydraulic Engineering**, 133: 39-47.

380

381

382

Lopez, F. and Garcia, M. (1998) open-channel flow through simulated vegetation: suspended sediment transport modelling. **Water Resour. Res**, 34: 2341-2352.

383

384

Nepf, H.M. (2012) Hydrodynamics of Vegetated Channels. **Journal of Hydraulic Research**, 50: (3): 262-279.

385

- 386 Nezu, I. and Nakagawa, H. (1984) Cellular Secondary Currents in Straight Conduit. **Journal**  
387 **of Hydraulic Engineering**, 110: 173-193.
- 388 Nezu, I. and Nakagawa, H. (1993) Turbulence in Open Channel Flows. **Rotterdam, A.A.**  
389 **Balkema**, (Rotterdam, A.A. Balkema).
- 390 Shiono, K. and Knight, D.W. (1991) Turbulent Open-Channel Flows with Variable Depth  
391 Across the Channel. **J. Fluid Mech**, 222: 617-646.
- 392 Shucksmith, J.D., Boxall, J.B. and Guymer, I. (2010) Effects of Emergent and Submerged  
393 Natural Vegetation on Longitudinal Mixing in Open Channels  
394 **Water Resources Research**, 46: (w04504): 1-14.
- 395 Wang, Z.-Q. and Cheng, N.-S. (2005) Secondary Flows Over Artificial Bed Strips. **Advances**  
396 **in Water Resources**, 28: 441-450.
- 397
- 398
- 399
- 400
- 401